Pertanika J. Sci. & Technol. 31 (5): 2453 - 2471 (2023)

PERTANIKA JOURNALS

SCIENCE & TECHNOLOGY

Journal homepage: http://www.pertanika.upm.edu.my/

A Comparison of the Performance of $MAPbI_3$ and $MASnI_3$ as an Inverted Perovskite Structure Using NiO as HTL Through Numerical GPVDM Simulation

Subathra Muniandy[1]*, Muhammad Idzdihar Idris[1], Zul Atfyi Fauzan Mohammed Napiah[1], Zarina Baharudin Zamani[1], Marzaini Rashid[2] and Luke Bradley[3]

[1]Faculty of Electronics and Computer Engineering, University Technical Malaysia Melaka (UTeM), 75450 Melaka, Malaysia
[2]School of Physics, University Science Malaysia, 11800 USM, Penang, Malaysia
[3]School of Engineering, Newcastle University, England

ABSTRACT

Perovskite solar cells (PSCs) are solar cells that have intriguing characteristics such as environmental friendliness and the capability for high power conversion efficiency, which have attracted study from both scientific investigation and analytical standpoints. However, lead toxicity has become a significant barrier to the widespread use of PSCs. Due to the serious environmental implications of lead, an environmentally compatible perovskite is required. Tin-based perovskite has a considerable impact, showing that it is a good hole extraction material with good mobility and low effective mass. In this study, we explore the impacts of perovskite and hole transporting layer (HTL) thickness, and intensity of light limitations, in inverted PSCs based on the structure of FTO/NiO/$MAPbI_3$/ZnO/Ag and FTO/NiO/$MASnI_3$/ZnO/Ag incorporating GPVDM (General-purpose Photovoltaic Device Model) to evaluate if $MASnI_3$ is a viable substitute to $MAPbI_3$. From the simulation results, the optimized parameters obtained for PCSs under 1 sun incorporating $MASnI_3$ were 27.97%, 0.88 a.u., 0.92 V, and 34.45 mA/cm^2. Instead, the optimized parameters obtained for PCSs incorporating $MAPbI_3$ were 24.94%, 0.88 a.u., 0.90 V, and 31.03 mA/cm^2. The thickness of the film of both PSC architectures was optimized to provide the best suitable result. The findings show that $MASnI_3$ is employed as a promising perovskite layer in PSCs instead of $MAPbI_3$.

Keywords: GPVDM software, $MAPbI_3$, $MASnI_3$, nickel oxide, perovskite solar cells

ARTICLE INFO

Article history:
Received: 01 September 2022
Accepted: 25 January 2023
Published: 21 July 2023

DOI: https://doi.org/10.47836/pjst.31.5.22

E-mail addresses:
m022020016@student.utem.edu.my (Subathra Muniandy)
idzdihar@utem.edu.my (Muhammad Idzdihar Idris)
zulatfyi@utem.edu.my (Zul Atfyi Fauzan Mohammed Napiah)
zarina@utem.edu.my (Zarina Baharudin Zamani)
marzaini@usm.my (Marzaini Rashid)
luke.bradley@strath.ac.uk (Luke Bradley)
*Corresponding author

Current Affiliation
Luke Bradley
Rolls Royce UTC, University of Strathclyde, Glasgow, Scotland, United Kingdom

ISSN: 0128-7680
e-ISSN: 2231-8526

INTRODUCTION

Solar energy offers several distinct benefits over other renewable energy sources, including the worldwide dispersion of sunshine and the decentralized nature of solar energy output (Mohtasham, 2015). Perovskite solar cells (PSCs) have emerged as the "third generation of solar cells," as alternative renewable energy to solve environmental implications such as global warming and greenhouse gases (Ibn-Mohammed et al., 2017). PSCs have been the most recent solar cell type and among the most promising thin-film PV technologies. Strong absorption coefficients, excellent charge carrier mobilities, diffusion duration, and solution processability are the desired properties that make perovskites a potentially new front-runner material for thin-film solar technology (Khadka et al., 2017). These qualities are required for their real implementation in semiconductor-based devices such as solar cells. Sustainable substitutes to present power-generating systems are critical to conserving the planetary environment by ensuring long-term economic prosperity. The recent discovery of halide perovskites as solar energy harvesting and hole-transport materials has contributed to the development of solar technology. Among the several types of PSCs, organic-inorganic metal halide PSCs have garnered substantial interest in recent years due to their high power conversion efficiency (PCE) and ease of fabrication at a cheap cost (Yongjin et al., 2020). The ABX_3 perovskite framework is used in organic-inorganic hybrid perovskite substances depending on metal halides. This architecture comprises networks of corner-sharing BX_6 octahedra, whereby B is a metal cation (usually Sn^{2+} or Pb^{2+}), and X is generally F^-, Cl^-, Br^-, or I^-. The A cation is used to equalize the overall charge or to represent a tiny molecular group (Hao et al., 2014). Methylammonium lead tri-iodide ($MAPbI_3$) has often been known to be a perovskite content and is widely employed in PSCs. Even though the efficiencies have now exceeded 20%, long-term stability is the major obstacle to commercializing PSCs on a broader level. As the lead in $MAPbI_3$ is extremely hazardous, industrial applications of $MAPbI_3$-based PSCs are severely limited (Conings et al., 2015; Wang, Phung et al., 2019; Wang, Mujahid et al., 2019), resulting in interest in lead-free PSCs in the sector of solar technologies.

Experts refer to the idea that inorganic halide perovskites, like Sn-, Ag-, Sb-, Bi-, Cu-, and Ge-based solar cells might be employed as lead substitutes (Green et al., 2014; Song et al., 2017). A tin-based perovskite, $MASnI_3$, is a possible option for lead-free PSCs owing to its excellent bandgap of 1.3eV, which are even narrower than $MAPbI_3$ (Baig et al., 2018). It was reported that $MASnI_3$ perovskite has high absorption efficiency with excellent optical features and the broadest light-absorption spectrum compared to $MAPbI_3$ (Du et al., 2016). Sn-based perovskites are environmentally beneficial since they decompose to SnO_2 (from Sn^{4+}) when exposed to air. Sn-based perovskites and Pb-based perovskites are comparable in their fundamental physical features (Ke & Kanatzidis, 2019; Schileo & Grancini, 2021). Vishnuwaran et al. (2022) have compared the performance of $MASnI_3$

and $FASnI_3$ perovskite materials. Modification in thickness and temperature of the absorber layer revealed that $MASnI_3$ had a higher cell efficiency (23.74%) than $FASnI_3$ (23.11%). Germanium (Ge) is another possible replacement for lead. Recent computational and experimental research has demonstrated that Ge–Sn mixtures are an excellent candidate for enhancing the performance of Ge^{2+}-based PSCs. Upon doping a tiny amount (5%) of Ge^{2+} into Ge–Sn mixed halide perovskites, an overall efficiency of 4.48% was attained (Vishnuwaran et al., 2022). The PCE grew to 6.9% after exposure to an N_2 environment for 72 hr. Simulation design and investigation of the performance of Sn-Ge-based perovskite in a planar inverter structure yield a PCE of 24.20%, such substantial enhancement established by trap density at the interface layers (Vishnuwaran et al., 2022). Furthermore, Pindolia et al. (2022) proposed an inorganic RbGeI3-based PSC that acquired an efficiency of 10.11% and a greater fill factor (FF) of 63.68% by analyzing alternative inorganic HTL and ETL layers. Like another example of Pb-free PSCs with great promise as light-absorbing perovskite, Cs2TiBr6, and Cs2PtI6 have a good absorption coefficient, a lengthy carrier lifespan, and outstanding stability with adequate bandgaps (1.8 eV and 1.4 eV, respectively). The value can be increased by refining the interface between perovskite and HTL. For this study, $MASnI_3$ was chosen and tested further as a potential replacement for lead-based PSCs.

Aside from the performance of perovskite material, the functionality and maximum efficiencies of PSCs are heavily influenced by the HTL. In the optimization of PSC, HTL can improve the overall performance of PSC by reducing series resistance, enhanced fill factor (FF), and open-circuit voltage (V_{OC}) while providing a transport medium for holes to the counter electrode (Yang et al., 2017). Owing to its improved chemical stability, cheap cost, and appropriate energy level, NiO, a direct bandgap inorganic material, has lately caught the scientific community's interest as a viable HTL for stable and efficient PSCs (Hossain et al., 2020). NiO is a significant transition metal oxide that may be easily deposited using a variety of processes, including spray pyrolysis (Danjumma, 2019), sputter deposition (Mulik, 2019), thermal decomposition (Guo et al., 2018), precipitation (Chowdhury et al., 2018), hot-casting (Abzieher et al., 2018), and electrodeposition (Xi et al., 2019). NiO demonstrated good potential in organic solar cells and has a work function of between 5 and 5.6 eV, which satisfies the criteria for an HTL (Nguyen, 2018). NiO, as a p-type semiconductor material, has been effectively used in PSCs with inverted architectures, according to its adequate carrier mobility and good work functionality, which can fit perovskite materials' energy (Chen et al., 2017). The energy band diagram reveals the good positioning of the NiO in such a way as to foster hole extraction from the perovskite material (Nkele et al., 2020). Besides that, there are already many research articles experimentally showing that NiO is a potential material for HTL with good efficiency of 17.75% (Thakur et al., 2020), 19.10% (Mali et al., 2018) and 20.8% (Mahmoudi et al., 2021) which undergone different synthesis processes. In previous work, the General-Objective

Photovoltaic Devices Model (GPVDM) has been used to determine the optimal material parameter for PSCs. GPVDM is a research-leading electrical and optical solver that the electrical transfer characteristics and the optical model pattern of PSCs (MacKenzie, 2016). The PCE of PSC was reported to increase from 9.96 to 12.9% through optimization of the layer thickness using this model (Hima et al., 2018). On the other hand, the effect of the thickness of $MAPbI_3$ as perovskite with Spiro-OMeTAD as HTL and different ETL material (TiO_2 and SiO_2) has a significant effect on overall PSC efficiency with reported values of 5.6%, 14.5%, and 14.7%, respectively (Mishra & Shukla, 2020; Abdulsalam et al., 2018; Yasodharan et al., 2019). The best-reported efficiencies were obtained with optimal 200 nm and 300 nm ETL thicknesses, respectively. A comparative study on the effect of perovskite layer thickness and charge mobilities in PSCs was also observed with an efficiency of 18.43% (Sittirak et al., 2019). The influence of light intensity has achieved an efficiency from 8.5 to 10%, which indicates that performance can be improved by maximizing the light falling on the solar cell's surface (Mekky, 2020).

There are more solar cell models besides GPVDM that investigate PSC-based structures with $MAPbI_3$, $MASnI_3$, NiO, and ZnO Rahman et al. (2019) used SCAPS-1D to construct a p-i-n structure with three distinct ETL layers (TiO_2, ZnO, and SnO_2) and compared their properties to that of $MAPbI_3$ as the perovskite layer and NiO as the HTL layer. The research proved that using ZnO as the ETL allowed for the highest possible PCE of 17.84%. The identical model was also used to simulate a $MASnI_3$-based PSC along with NiO as the HTL and PCBM as the ETL to study the details of the device by changing the layer thickness, defect density at junctions, density of states, and metalwork efficiently (Shamna et al., 2020). It is estimated from the simulation result that the designed structure has attained an efficiency of 22.95% with the optimal absorber layer thickness of 600 nm. Another study used the Silvaco ATLAS device model to construct a lead-free titanium PSC (Cs_2TiBr_6) using TiO_2 as the ETL and comparison of three HTLs (CuPc, P_3HT, and NiO), in which NiO gaining the maximum PCE of 8.5% (Samanta et al., 2020). Although the efficiency of Cs_2TiBr_6 based-PSC is poor compared to lead-based PSCs, its long-term stability and, most significantly, its eco-friendly nature are predicted to drive it to the forefront of future solar cell application. In addition, Karimi et al. (2020) performed a comparative analysis of the SCAPS and AMPS software applications to explore the impact of ZnO and SnO_2 on PSC performances.

Aside from NiO as HTL, many inorganic materials are discovered as HTL layers to study the performance of lead-free PSCs. Anand Kumar Singh et al. (Singh et al., 2021) conducted a simulation study that focuses on $MASnI_3$ perovskite sandwiched between CuO_2 as HTL and TiO_2 as ETL, achieving maximum efficiency of 27.43% by varying various parameters with the aid of SCAPS-1D simulator. CZTS has recently been analyzed as HTL in tin-based PSC by optimizing layer thickness, energy bandgap, and operating temperature that acquire the best PCE of 20.28% (Reyes et al., 2021). For the first time, the inorganic

material $CuSbS_2$ was employed as HTL in alignment with the $MASnI_3$ as the active layer, and the resulting device achieved an efficiency of 24.1% and further boosting the doping concentration of $MASnI_3$ contributed to an increase in PCE value. (Devi & Mehra, 2019). According to the literature review, inorganic materials are now well-equipped to replace the costly Spiro-MeOTAD and demonstrate the potential to become the ideal alternative for use in the future. Several solvers programs are available, including open source and subscription to model and simulate solar cells. At the same time, certain simulation software shares a common module but varies in terms of speed, features, the quality of the user interfaces, and how easy or difficult to use (Kowsar et al., 2019). It is important to note that this study used an optimized configuration that achieved the highest possible efficiency of 27.43%, the maximum value documented for this configuration by GPVDM simulation software.

From previous work, factors such as the thickness of the film, carrier mobilities, defect density, and light intensity influence device performance optimization. This work investigated the effect of PSCs on the configuration of $MASnI_3$, which was investigated through GPVDM simulations. During the simulations, the thickness of perovskite, the thickness of HTL, and the light intensity were varied to attain the optimal values to maximize the PCE. A comprehensive analysis of the electrical and optical characteristics affecting each performance of $MASnI_3$ and $MAPbI_3$ as perovskite with NiO as HTL has never been described. Furthermore, the results of this inquiry may be extremely valuable and give excellent direction for the understanding of the acquired data, which will aid in revealing the primary processes of PCE rise in the structure of $MASnI_3$ as perovskite and NiO as HTL.

METHODOLOGY

In Figure 1, the device comprises a layered configuration made from an inverted planar structure (FTO/NiO/Perovskite/ZnO/Ag). Two absorbance layers were compared as the primary carrier producer ($MASnI_3$ and $MAPbI_3$). P-type (HTL = NiO) and n-type (ETL = ZnO) were placed on the top and bottom perovskite layers. The close boundary conditions were applied to the simulation environment, where fluorine tin oxide (FTO) was selected as a glass substrate and silver (Ag) was chosen as the back-electrode layer designated as anode and cathode, respectively. The simulation studies in this work were performed using the GPVDM tool, a freeware solar cell modeling software for photovoltaic systems. The model captures the joint movement of electrons, holes, and transport momentum equation in the orientated area to reflect the movement of loads within the device. The GPVDM software often only provides specialized simulation materials. The NiO, $MAPbI_3$, and $MASnI_3$ material was manually introduced to the GPVDM software following the technique in (MacKenzie, 2016). The absorption and refractive index data of NiO, $MAPbI_3$, and $MASnI_3$ were extracted from the previous work reported by Bakr et al. (2015) and Sun et

al. (2016). This work focuses much on the perovskite and HTL layer, which were largely set to evaluate their effectiveness as active layers.

Both device structure was simulated under one sun AM 1.5G illumination (1 kW/m^2; T = 300°K). Table 1 summarizes the designed default GPVDM software variables used during the simulation. The physical parameters of $MAPbI_3$ and $MASnI_3$, such as bandgap (Eg), electron affinity (Xi), density electron states (cm^{-3}), density hole states (cm^{-3}), electron mobility (cm^2/Vs), hole mobility (cm^2/Vs) and relative permittivity (Ɛr) were taken from previous experimental and simulation studies (Ahmed et al., 2019; Mohammadi et al., 2021; Hima et al., 2018; Then et al., 2021). Three different approaches were performed to find the optimum parameters of the solar cell, which are (1) different thicknesses of perovskite layer ranging from 50 to 500 nm, (2) different thicknesses of HTL layer varying from 100 to 800 nm, and (3) different values of light intensity. The activated perovskite layer and HTL layer have quite a significant effect on the efficiency of the cells.

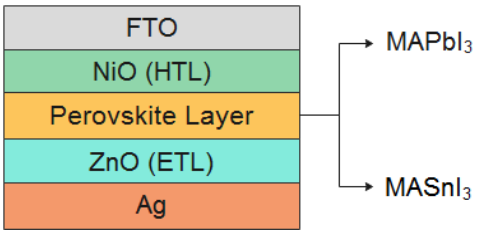

Figure 1. Schematic representation of inverted PSCs with $MASnI_3$ and $MAPbI_3$ perovskite material

RESULTS AND DISCUSSION

Optimization of the perovskite layer thickness is one of the approaches for increasing the PCE. A sufficient thickness is necessary for a successful perovskite device to achieve enough light absorbance and effective charge carrier capture. A perovskite is sufficiently thick in the region of its absorption; then, it leads to an excellent photovoltaic performance (Iakobson et al., 2021; Rai et al., 2020). The thickness of the perovskite film plays an essential part in the device for optimal carrier generation. The influence of perovskite film thickness on cell efficiency was evaluated by computational

Table 1

Simulation parameter of both perovskite layers and NiO (Ahmed et al., 2019; Du et al., 2016; Hao et al., 2014)

No.	Parameters	Layers		
		$MAPbI_3$	$MASnI_3$	NiO
1.	Bandgap energy, Eg (eV)	1.55	1.3	1.46
2.	Electron affinity, Xi (eV)	3.93	4.17	3.80
3.	Density electron states (cm^{-3})	$1.3x10^{26}$	$1x10^{18}$	-
4.	Density hole states (cm^{-3})	$9.1x10^{26}$	$1x10^{18}$	$1x10^{18}$
5.	Electron mobility (cm^2/Vs)	$2x10^{-1}$	$2x10^{-2}$	2.8
6.	Hole mobility (cm^2/Vs)	$2x10^{-1}$	$2x10^{-4}$	2.8
7.	Relative permittivity, Ɛr	6.5	8.2	11.7

models, with a thickness range of 50 to 500 nm (Yasodharan et al., 2019). According to Figures 2(a) and 2(d), the PSC with the $MASnI_3$ has the maximum PCE of 12.88% and J_{SC} of 16.74 (mA/cm^2), whereas the PSC with the $MAPbI_3$ has the greatest PCE of 16.96% and J_{SC} of 22.53 (mA/cm^2). The higher the thickness of the perovskite layer, the greater the performance of PCE produced.

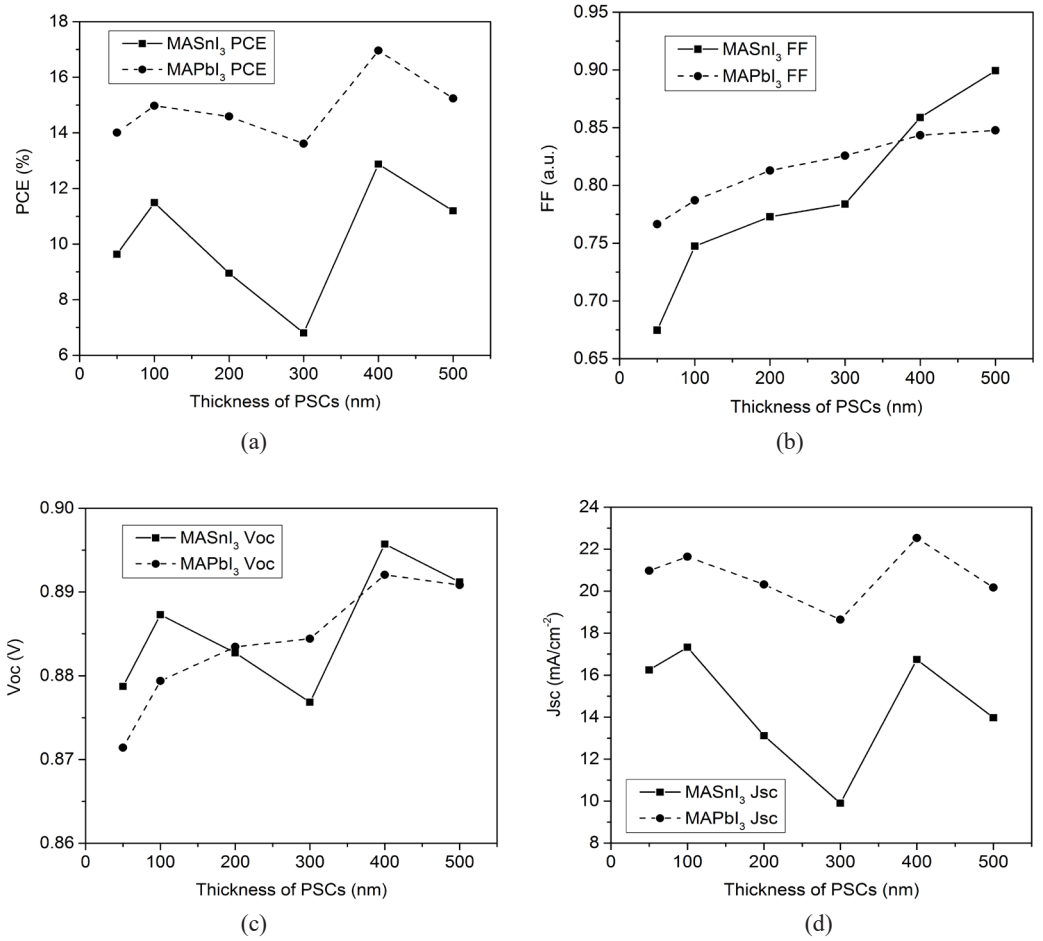

Figure 2. The optimized outcome of perovskite thickness generated by the GPVDM software focusing on the comparison between $MASnI_3$ and $MAPbI_3$ produced at 400 nm of (a) PCE, (b) FF, and (c) V_{OC}, and (d) J_{SC}

The thickness of the perovskite layer increases slowly from 50 to 100 nm, and after that, it decreases when approaching to 200 to 300 nm thickness range. It causes an abrupt drop in the V_{OC} for both perovskite layers (Figure 2c). In contrast, the PCE and J_{SC} showed the highest value at the thickness of 400 nm. It explains how, after the perovskite has reached its ideal thickness, it regulates the interfacial structuring to improve light trapping, resulting in a greater carrier concentration and, as an outcome, a higher J_{SC} (Rai et al., 2020). It is

important to mention that even though the computed J_{SC} for the $MASnI_3$ perovskite device is less efficient than that for the $MAPbI_3$ device, the greatest current density above 15 mA/cm^2 can be achieved when integrating $MASnI_3$ perovskite under the bandgap of the 1.30 eV. However, at the thickness of 500 nm, there is also a small significant decrease in PCE and V_{OC}. In contrast to PCE and $V_{OC,}$ the outcome of FF keeps increasing with perovskite thicknesses from 50 to 500 nm (Figure 2b). It is due to the thicker perovskite layer that absorbs more significant photons using broader wavelengths, thus increasing the production of electron and hole pairs (Lin et al., 2017).

Although the PCE of $MASnI_3$ is lower compared to $MAPbI_3$, the FF of $MASnI_3$ is larger, which implies lower recombination at the interface. The V_{OC} also constantly increased as the thickness of the perovskite layer increased but dropped when it reached 500 nm, as shown in Figure 2(c). It is also the same case with the simulation study made by Hima et al. (2019), which shows that the PCE drops after the thickness of the perovskite layer reaches the optimal value at 600 nm. As the thickness of the perovskite approached its optimal value, the recombination rate increased, and the efficiency of the cell decreased as a consequence.

In addition, the current simulation study shows much better results than the preceding simulation results using $MAPbI_3$ as a perovskite in GPVDM, which were obtained about 12.83% at 200 nm (Hima et al., 2018) and 14.7% at 300nm (Abdulsalam et al., 2018). Instead, Ahmed et al. (2019) reported that the performance hit as much as 20% at a thickness of 850 nm. A thicker layer of perovskite causes it difficult for charge carriers created by photons to be carried away, reducing the device's effectiveness. This statement also agreed with the report by Nam et al. (2010) about bulk heterojunction organic solar cells and Sievers et al. (2006) regarding polymer bulk-heterojunction solar cells. The optimal thickness should be determined by a balance between the absorption range and the diffusion length of the material (Ragb et al., 2021). Besides that, the obtained result showed higher efficiency than the experimental result of Srivastava et al. (2021), using $MAPbI_3$ perovskite with obtained PCE of 14.44%. Another report also focuses on fabricating $MAPbI_3$ perovskite achieved an efficiency of 14.79% with regulated moisture of 35% in ambient air using a one-step spin coating method (Soucase et al., 2022). In conjunction, solution-processed PSCs based on $MASnI_3$ as the light-absorbing material achieved a PCE of 5.8% (Hao et al., 2014). Based on the analysis between $MAPbI_3$ and $MASnI_3$, the thickness of the perovskite layer plays a major role in increasing the performance of the photovoltaic device (Bag et al., 2020). Additionally, this work obtained efficiency much higher than the experimental outcome, which recently studied NiO nanocrystal film as HTL for Sn-Pb-based PSCs with PCE up to 18.8% (Chen et al., 2021).

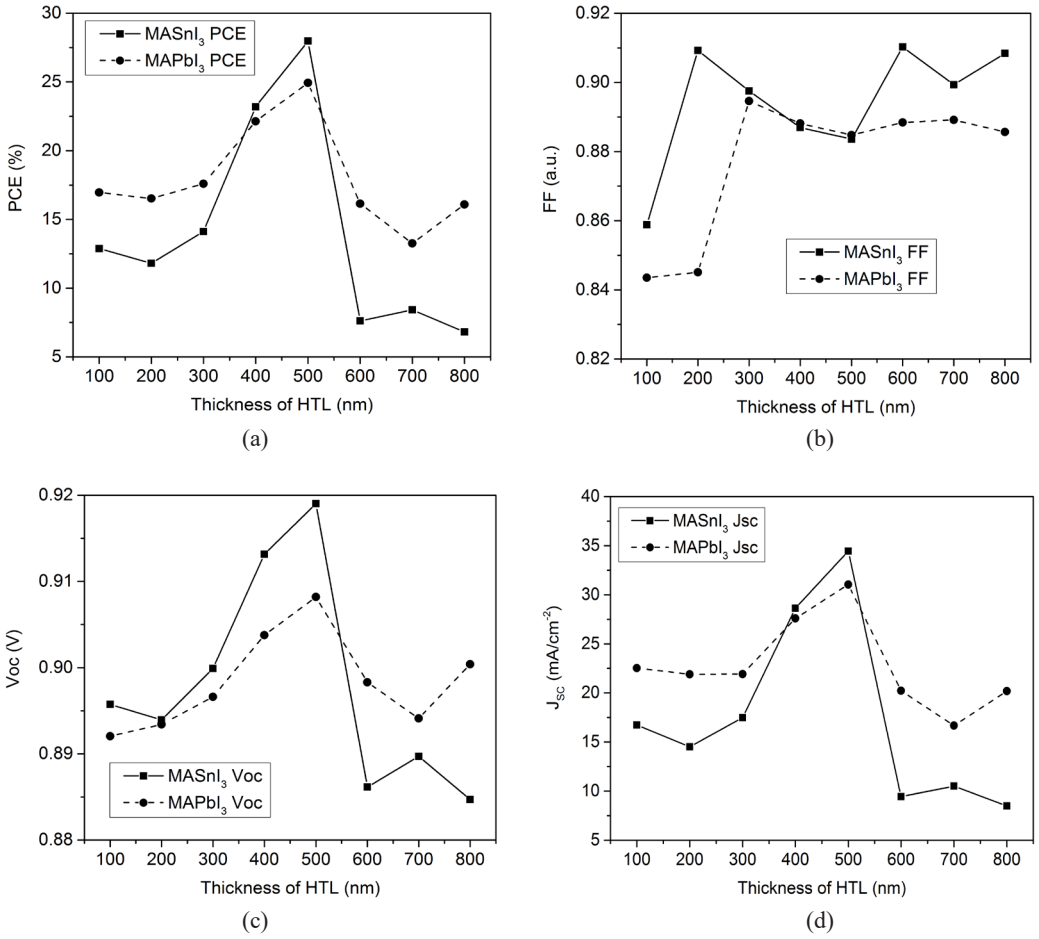

Figure 3. The optimized thickness of NiO as HTL generated by the GPVDM software focusing on the comparison of $MASnI_3$ and $MAPbI_3$ obtained at 500 nm of (a) PCE, (b) FF, (c) V_{OC}, and (d) J_{SC}

Additionally, the impact of light intensity on each solar cell affects all electrical parameters. The quantity of 1 Suns indicates the normal AM1.5 or 1 (kW/m^2) lighting on a PSC. Equally, a solar cell system with 10 (kW/m^2) could run at 10 suns. The PCE of $MASnI_3$ is much higher than that of $MAPbI_3$, which is at 29.90% and 26.67%, as seen in Figure 4(a). The growing levels of PCE were seen for both materials as the intensity of the light increased up to 10 (kW/m^2), which has been previously found in Mekky (2020) utilizing a hybrid perovskite-based solar cell employing a GPVDM model. The above findings indicate that the PCE relies on light-intensity instances and exhibits an extraordinary increase in light-intensity energy transformation. The same trend was also observed in the graph of Figure 4(c); as the intensity of the light increased, the V_{OC} also kept increasing, which is similarly reported by Liu et al. (2017) using $MAPbI_3$ as a perovskite layer.

In contrast, the FF is mainly influenced by the amount of light intensity (Figure 4b). Both structure FF rise when the light intensity is less than 1 kW/m^2. However, when the intensity of the light hits more than 1 kW/m^2, the FF decreases owing to the impact of series resistance (Mekky, 2020). Figure 4(d) illustrates that the J_{SC} from a solar cell depends linearly on the light intensity, such that a device operating under 10 suns would have 10 times the J_{SC} as the same device under one sun operation. However, this effect does not increase efficiency since the incident power also increases linearly. Instead, the efficiency benefits arise from the dependence of the V_{OC} on short circuits. Subsequently, the same trend of J_{SC} was observed by Kassahun Lewetegn Damena through GPVDM in which the light intensity was varied from 1 sun to 40 suns (Damena, 2019).

The J–V curves of the devices were illustrated in Figure 5, recorded the $MASnI_3$ perovskite-based solid-state device exhibits the highest mean J_{SC} of 32.05 mA/cm^2 and

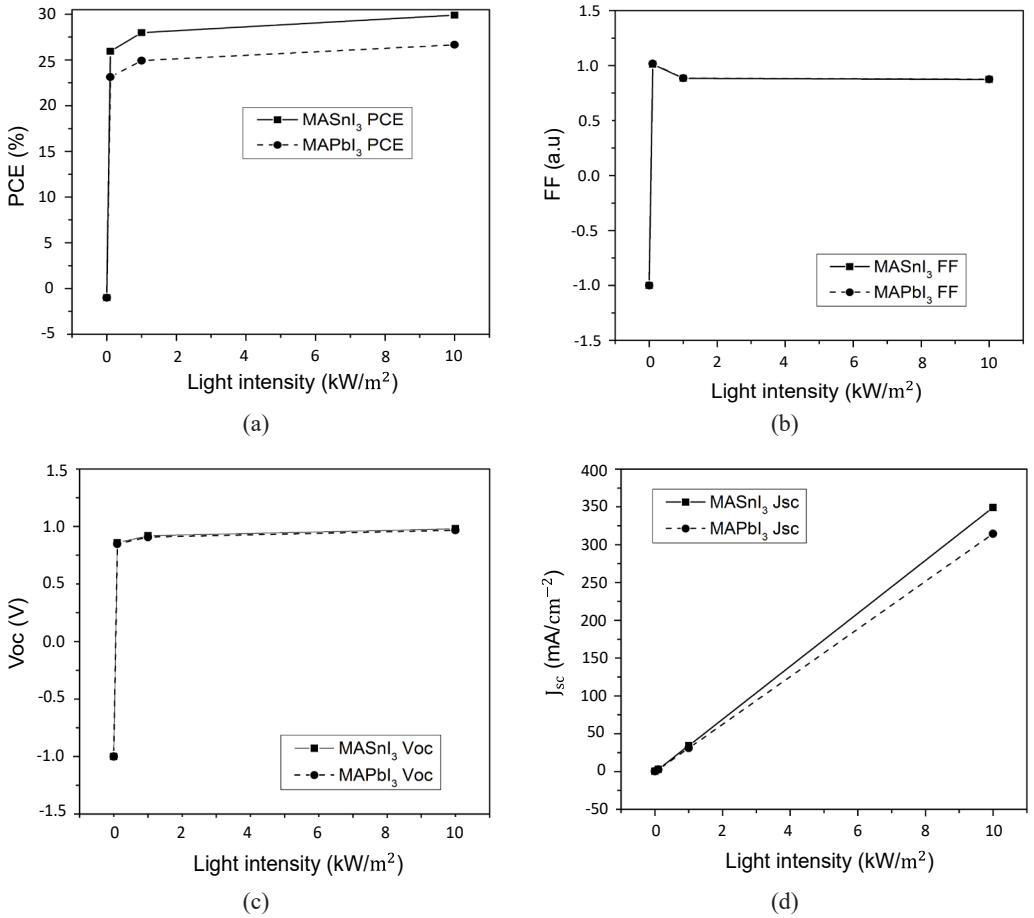

Figure 4. The influence of light intensity on $MASnI_3$ and $MAPbI_3$ perovskite achieved an optimum value at 10 (kW/cm^2) of (a) PCE, (b) FF, (c)V_{OC}, and (d) J_{SC}

V_{OC} of 1.6 V under AM 1.5G solar illumination. Meanwhile, the $MAPbI_3$ device showed a slightly lower J_{SC} of 27.93 mA/cm^2 and V_{OC} of 1.2 V. A substantial rise in V_{OC} was detected in the $MASnI_3$ device compared to the $MAPbI_3$ device. The current analysis also demonstrates the potential ability of tin-based perovskite contrasted with lead-based perovskite. Previously, Mandadapu et al. (2017) presented a simulation regarding $MASnI_3$ PSC with the thickness of 600 nm obtained PCE, J_{SC}, and V_{OC} of 24.82 %, 25.67 mA/cm^2 and 1.04 V correspondingly. Nevertheless, another simulation study of $MASnI_3$ compared to $MAPbI_3$ reported by Shyma and Sellappan (2021) gained an efficiency of 24.3 % with J_{SC} of 32.30 mA/cm^2, which is higher than the current study yet still shows a lower V_{OC} of 1.2 V. Regardless of the simulation studies, Li et al. (2019) demonstrated an experimental result of $MASnI_3$ developed using a two-step technique for the deposition of solid and homogeneous perovskite layers, reaching the optimum value of PCE at 7.13 %, J_{SC} at 22.91 mA/cm^2 and V_{OC} at 0.486 V.

It is well known that the present simulation result of $MASnI_3$ PSC has enhanced the photovoltaic performances of the devices compared to the $MAPbI_3$ PSC. It can be supported by the fact that by integrating the AM 1.5G solar spectrum below the bandgap of $MASnI_3$ (1.30 eV) perovskite, the greatest current density that can be produced, despite the lower J_{SC} found for $MAPbI_3$ perovskite (Hao et al., 2014). Besides that, this could be owing to the perovskite's wide optical absorbance cross-section and the well-developed interstitial pore opening by the hole conductor, which allowed for this tremendous current density produced by $MASnI_3$ (Cao & Yan, 2021; Du et al., 2016). Additionally, the insertion of the NiO HTL in the structure significantly improves the PCE of the solar cells, which is attributed due to the suitable band alignment of the NiO and perovskite.

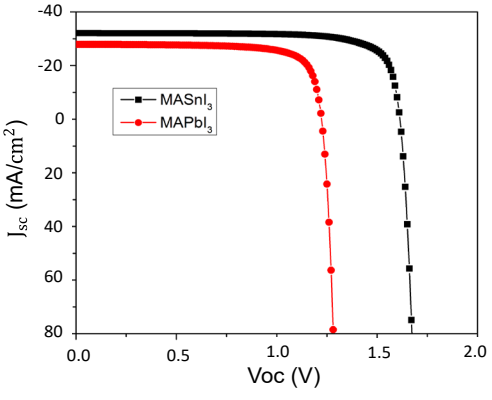

Figure 5. The optimized curve of photocurrent density-voltage (J-V) achieved higher by $MASnI_3$ at J_{SC} of 32.05 mA/cm^2 and V_{OC} of 1.6 V in parallel with $MAPbI_3$ obtained at J_{SC} of 27.93 mA/cm^2 and V_{OC} of 1.2 V as perovskite

The photon density distribution corresponding wavelength as a function of the position of the $MAPbI_3$ device layers was presented in Figure 6(a). Most photons are absorbed in the perovskite absorbance layer. Therefore, massive electrons and holes have promoted the device's efficiency (Said & Woon, 2019). The same trend was also observed for the $MASnI_3$ PSC in Figure 6(b). The photon of both PSCs was more significant from FTO and decreased after the Ag electrode was incorporated. When the light penetrates an absorber layer of the film, the process of pumping electrons through the valence band into the conduction band

occurs. The electrons quickly start to move to the ETL of the n-type ZnO, whereas the holes begin to migrate to the HTL of the p-type NiO. The ZnO has a lower work function (−4.4 eV) which matches with the lowest unoccupied molecular orbital (LUMO) energy level of $MAPbI_3$ perovskite film (LUMO = −3.9 eV) and $MASnI_3$ perovskite film (LUMO = −4.2 eV). The band structure of perovskite/ZnO further accelerates the electron transport to the Ag cathode (LUMO = −4.3 eV). NiO work function (-5.3 eV) must be aligned as closely as possible with the highest molecular orbital (HOMO) energy level of the ITO (HOMO = −4.0 eV) to deliver accurate hole direction. The minority and majority carriers are generated when a photon is absorbed. Absorbed photons at the HTL interface (NiO) showed that the $MASnI_3$ structure absorbs higher than the $MAPbI_3$ structure but decreases in time. It indicates that the stored charge at the hole-extracting interface of NiO could have a strong downward band bending on the perovskite side at the perovskite/HTL interface (Ravishankar et al., 2019). It is consistent with that tin-based perovskite produces the highest efficiency levels. The resulting shift of NiO in the work function leads to a more beneficial energy level alignment with the $MASnI_3$ perovskite, which is believed to facilitate charge extraction. Therefore, the photovoltaic performance is enhanced by an appropriate work function in relation to the perovskite interfaces. The downward band bending is potentially detrimental to charge extract and recombination kinetics because it sends holes back to the perovskite surface, which could increase the device's performance. The driving energy for hole injection happens from the valence band maximum of the HTL and should be greater in energy than the valence band maximum of the perovskite (Haider et al., 2022).

However, the photon density produced at the $MAPbI_3$ interface is higher than at the $MASnI_3$ interface. The $MAPbI_3$ perovskites have much higher radiative recombination coefficients, leading to the situation that $MASnI_3$ is much less charge carrier densities faced in photovoltaic at intensities around 1 sun (Kirchartz, 2019). Therefore, only a small percentage of photons will be created within the interface of $MASnI_3$.

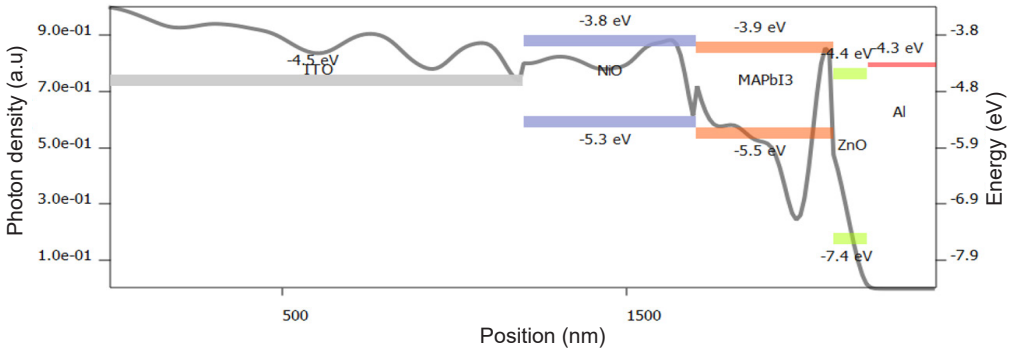

(a)

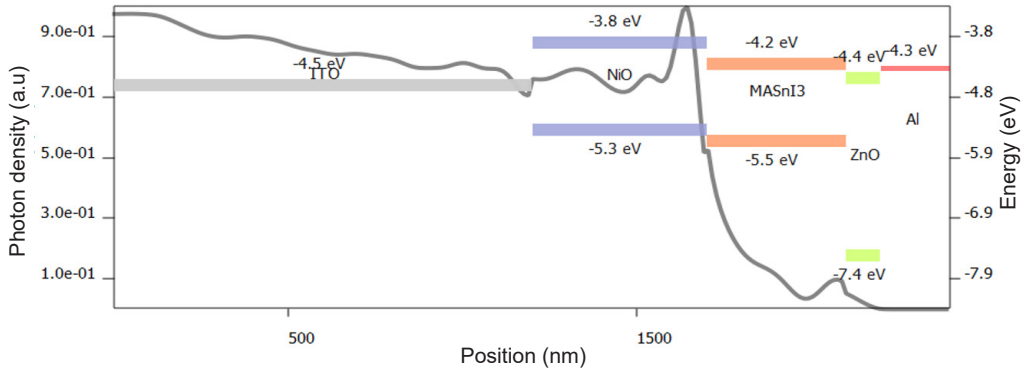

(b)

Figure 6. Photon density distributions (a) $MAPbI_3$ and (b) $MASnI_3$ as perovskite with the AM 1.5G solar spectrum interfaced with the thickness of the device

CONCLUSION

In summary, tin-based perovskites have excellent optoelectronic properties which lead to a promising candidate for efficient lead-free PSCs. Under 1 sun light intensity the tin-based perovskites have achieved the highest PCE of 27.97% while the lead-based perovskite achieved PCE at 24.94% using GPVDM software. During the optimization of perovskite layer thickness both perovskite material found at 400 nm in which the higher efficiency was attained by lead-based perovskite. Nevertheless, after the evaluation made on the HTL thickness the highest efficiency was noticed on tin-based perovskites at 500 nm with high J_{SC} and V_{OC} value. The findings imply that lead-free $MASnI_3$ has a huge potential as an absorber layer when combined with a robust inorganic hole transport material like NiO. Moreover, further increase of light intensity in each structure implies a progressive increase in PCE. Encouragingly, simulation models produced a maximum PCE of more than 20% that can be achieved from tin-based PSCs under optimized conditions. A deeper study on the previous simulation and experimental of each of the photovoltaic parameters such as PCE, J_{SC}, $V_{OC,}$ and FF reveals that the Sn-based devices perform better for high efficiency in lead-free PSC. In comparison to, lead-based counterparts, tin-based PSCs have a higher V_{OC} with a record value of 1.6 V, which consider higher than previous studies. Importantly, these computational results demonstrate that the absorber and HTL layers significantly impact system efficiency. The construction of a high-efficiency tin-based PSCs will be aided by this simulation study.

ACKNOWLEDGMENTS

This work was supported by the Ministry of Higher Education Malaysia and the Technical University of Malaysia Melaka through the Fundamental Research Grant Scheme with

Project No FRGS/1/2020/FKEKK-CETRI/F00423 and PJP/2021/FTKEE/S01822. The author also acknowledges the provider of the free version of GPVDM software.

REFERENCES

Abdulsalam, H., Babaji, G., & Abba, H. T. (2018). The effect of temperature and active layer thickness on the performance of CH3NH3PbI3 perovskite solar cell: A numerical simulation approach. *Journal for Foundations and Applications of Physics*, *5*(2), 141-151. http://sciencefront.org/ojs/index.php/jfap/article/download/89/58

Abzieher, T., Schwenzer, J. A., Sutterluti, F., Pfau, M., Lotter, E., Het-terich, M., Lemmer, U., Powalla, M., & Paetzold, U. W. (2018). Towards inexpensive and stable all-evaporated perovskite solar cells for industrial large-scale fabrication. In *2018 IEEE 7th World Conference on Photovoltaic Energy Conversion (WCPEC)(A Joint Conference of 45th IEEE PVSC, 28th PVSEC & 34th EU PVSEC)* (pp. 2803-2807). IEEE Publishing. https://doi.org/10.1109/PVSC.2018.8547364

Ahmed, S., Shaffer, J., Harris, J., Pham, M., Daniel, A., Chowdhury, S., Ali, A., & Banerjee, S. (2019). Simulation studies of non-toxic tin-based perovskites: Critical insights into solar performance kinetics through comparison with standard lead-based devices. *Superlattices and Microstructures*, *130*, 20-27. https://doi.org/10.1016/j.spmi.2019.04.017

Bag, A., Radhakrishnan, R., Nekovei, R., & Jeyakumar, R. (2020). Effect of absorber layer, hole transport layer thicknesses, and its doping density on the performance of perovskite solar cells by device simulation. *Solar Energy*, *196*, 177-182. https://doi.org/10.1016/j.solener.2019.12.014

Baig, F., Khattak, Y. H., Mari, B., Beg, S., Ahmed, A., & Khan, K. (2018). Efficiency enhancement of $CH_3NH_3SnI_3$ solar cells by device modeling. *Journal of Electronic Materials*, *47*, 5275-5282. https://doi.org/10.1007/s11664-018-6406-3

Bakr, N. A., Salman, S. A., & Shano, A. M. (2015). Effect of co doping on structural and optical properties of NiO thin films prepared by chemical spray pyrolysis method. *International Letters of Chemistry, Physics and Astronomy*, *41*, 15-30. https://doi.org/10.56431/p-k5woe6

Cao, J., & Yan, F. (2021). Recent progress in tin-based perovskite solar cells. *Energy & Environmental Science*, *14*(3), 1286-1325. https://doi.org/10.1039/d0ee04007j

Chen, H., Peng, Z., Xu, K., Wei, Q., Yu, D., Han, C., Li, H., & Ning, Z. (2021). Band alignment towards high-efficiency NiOx-based Sn-Pb mixed perovskite solar cells. *Science China Materials*, *64*(3), 537-546. https://doi.org/10.1007/s40843-020-1470-5

Chen, W., Liu, F. Z., Feng, X. Y., Djurišić, A. B., Chan, W. K., & He, Z. B. (2017). Cesium doped NiOx as an efficient hole extraction layer for inverted planar perovskite solar cells. *Advanced Energy Materials*, *7*(19), Article 1700722. https://doi.org/https://doi.org/10.1002/aenm.201700722

Chowdhury, M. S., Shahahmadi, S. A., Chelvanathan, P., Tiong, S. K., Amin, N., Techato, K., Nuthammachot, N., Chowdhury, T., & Suklueng, M. (2020). Effect of deep-level defect density of the absorber layer and n/i interface in perovskite solar cells by SCAPS-1D. *Results in Physics*, *16*, Article 102839. https://doi.org/10.1016/j.rinp.2019.102839

Chowdhury, T. H., Kaneko, R., Kayesh, M. E., Akhtaruzzaman, M., Sopian, K. B., Lee, J. J., & Islam, A. (2018). Nanostructured NiOx as hole transport material for low temperature processed stable perovskite solar cells. *Materials Letters*, *223*, 109-111. https://doi.org/10.1016/j.matlet.2018.04.040

Conings, B., Drijkoningen, J., Gauquelin, N., Babayigit, A., D'Haen, J., D'Olieslaeger, L., Ethirajan, A., Verbeeck, J., Manca, J., Mosconi, E., Angelis, F. D., & Boyen, H. G. (2015). Intrinsic thermal instability of methylammonium lead trihalide perovskite. *Advanced Energy Materials*, *5*(15), Article 1500477. https://doi.org/10.1002/aenm.201500477

Damena, K. L. (2019). Investigation of organic solar cell at different active layer thickness and suns using GPVDM. *International Research Journal of Engineering and Technology*, *6*(12), 1615-1626. https://www.irjet.net/archives/V6/i12/IRJET-V6I12284.pdf

Devi, C., & Mehra, R. (2019). Device simulation of lead-free $MASnI_3$ solar cell with $CuSbS_2$ (copper antimony sulfide). *Journal of Materials Science*, *54*, 5615-5624. https://doi.org/10.1007/s10853-018-03265-y

Du, H. J., Wang, W. C., & Zhu, J. Z. (2016). Device simulation of lead-free $CH_3NH_3SnI_3$ perovskite solar cells with high efficiency. *Chinese Physics B*, *25*(10), Article 108802. https://doi.org/10.1088/1674-1056/25/10/108802

Green, M. A., Ho-Baillie, A., & Snaith, H. J. (2014). The emergence of perovskite solar cells. *Nature Photonics*, *8*, 506-514. https://doi.org/10.1038/nphoton.2014.134

Guo, Y., Yin, X., Liu, J., Yang, Y., Chen, W., Que, M., Que, W., & Gao, B. (2018). Annealing atmosphere effect on Ni states in the thermal-decomposed NiOx films for perovskite solar cell application. *Electrochimica Acta*, *282*, 81-88. https://doi.org/10.1016/j.electacta.2018.06.019

Haider, M. I., Fakharuddin, A., Ahmed, S., Sultan, M., & Schmidt-Mende, L. (2022). Modulating defect density of NiO hole transport layer via tuning interfacial oxygen stoichiometry in perovskite solar cells. *Solar Energy*, *233*, 326-336. https://doi.org/10.1016/j.solener.2022.01.023

Hao, F., Stoumpos, C. C., Cao, D. H., Chang, R. P. H., & Kanatzidis, M. G. (2014). Lead-free solid-state organic--inorganic halide perovskite solar cells. *Nature Photonics*, *8*(6), 489-494. https://doi.org/10.1038/nphoton.2014.82

Hima, A., Khechekhouche, A., Kemerchou, I., Lakhdar, N., Benhaoua, B., Rogti, F., Telli, I., & Saadoun, A. (2018). GPVDM simulation of layer thickness effect on power conversion efficiency of $CH_3NH_3PbI_3$ based planar heterojunction solar cell. *International Journal of Energetica*, *3*(1), 37-41. https://doi.org/10.47238/ijeca.v3i1.64

Hima, A., Khouimes, A. K. L., Rezzoug, A., Yahkem, M. B., Khechekhouche, A., & Kemerchou, I. (2019). Simulation and optimization of $CH_3NH_3PbI_3$ based inverted planar heterojunction solar cell using SCAPS software. *International Journal of Energetica*, *4*(1), 56-59. https://doi.org/10.47238/ijeca.v4i1.92

Hossain, M. I., Hasan, A. K. M., Qarony, W., Shahiduzzaman, M., Islam, M. A., Ishikawa, Y., Uraoka, Y., Amin, N., Knipp, D., Akhtaruzzaman, M., & Tsang, Y. H. (2020). Electrical and Optical Properties of Nickel-Oxide Films for Efficient Perovskite Solar Cells. *Small Methods*, *4*(9), Article 2000454. https://doi.org/10.1002/smtd.202000454

Iakobson, O. D., Gribkova, O. L., Tameev, A. R., & Nunzi, J. M. (2021). A common optical approach to thickness optimization in polymer and perovskite solar cells. *Scientific Reports*, *11*, Article 5005. https://doi.org/10.1038/s41598-021-84452-x

Ibn-Mohammed, T., Koh, S. C. L., Reaney, I. M., Acquaye, A., Schileo, G., Mustapha, K. B., & Greenough, R. (2017). Perovskite solar cells: An integrated hybrid lifecycle assessment and review in comparison with other photovoltaic technologies. *Renewable and Sustainable Energy Reviews*, *80*, 1321-1344. https://doi.org/10.1016/j.rser.2017.05.095

Karimi, E., & Ghorashi, S. M. B. (2020). The effect of SnO_2 and ZnO on the performance of perovskite solar cells. *Journal of Electronic Materials*, *49*, 364-376. https://doi.org/10.1007/s11664-019-07804-4

Ke, W., & Kanatzidis, M. G. (2019). Prospects for low-toxicity lead-free perovskite solar cells. *Nature Communications*, *10*, Article 965. https://doi.org/10.1038/s41467-019-08918-3

Khadka, D. B., Shirai, Y., Yanagida, M., Ryan, J. W., & Miyano, K. (2017). Exploring the effects of interfacial carrier transport layers on device performance and optoelectronic properties of planar perovskite solar cells. *Journal of Materials Chemistry C*, *5*(34), 8819-8827. https://doi.org/10.1039/C7TC02822A

Kim, G. W., Shinde, D. V, & Park, T. (2015). Thickness of the hole transport layer in perovskite solar cells: performance versus reproducibility. *RSC Advances*, *5*(120), 99356-99360. https://doi.org/10.1039/c5ra18648j

Kirchartz, T. (2019). Photon management in perovskite solar cells. *Journal of Physical Chemistry Letters, 10*(19), 5892-5896. https://doi.org/10.1021/acs.jpclett.9b02053

Kowsar, A., Billah, M., Dey, S., Debnath, S. C., Yeakin, S., & Uddin Farhad, S. F. (2019). Comparative Study on Solar Cell Simulators. In *2019 2nd International Conference on Innovation in Engineering and Technology (ICIET)* (pp 1-6). IEEE Publishing. https://doi.org/10.1109/ICIET48527.2019.9290675

Lee, M. M., Teuscher, J., Miyasaka, T., Murakami, T. N., & Snaith, H. J. (2012). Efficient hybrid solar cells based on meso-superstructured organometal halide perovskites. *Science*, *338*(6107), 643-647. https://doi.org/10.1126/science.1228604

Li, F., Zhang, C., Huang, J. H., Fan, H., Wang, H., Wang, P., Zhan, C., Liu, C. M., Li, X., Yang, L. M., Song, Y., & Jiang, K. J. (2019). A Cation-Exchange approach for the fabrication of efficient methylammonium tin iodide perovskite solar cells. *Angewandte Chemie International Edition*, *58*(20), 6688-6692. https://doi.org/10.1002/anie.201902418

Lin, L., Jiang, L., Qiu, Y., & Yu, Y. (2017). Modeling and analysis of HTM-free perovskite solar cells based on ZnO electron transport layer. *Superlattices and Microstructures*, *104*, 167-177. https://doi.org/10.1016/j.spmi.2017.02.028

Liu, M., Endo, M., Shimazaki, A., Wakamiya, A., & Tachibana, Y. (2017). Light intensity dependence of performance of lead halide perovskite solar cells. *Journal of Photopolymer Science and Technology*, *30*(5), 577-582. https://doi.org/10.2494/photopolymer.30.577

Nguyen, L. (2018). *New Method of Nickel Oxide as Hole Transport Layer and Characteristics of Nickel Oxide Based Perovskite Solar Cell* [Master dissertation]. Old Dominion University, USA. https://doi.org/10.25776/8dx3-kz45

MacKenzie, R. C. (2022). *Gpvdm user manual v7.88*. http://www.gpvdm.com/docs/man/man.pdf

Mahmoudi, T., Wang, Y., & Hahn, Y.-B. (2021). Highly stable perovskite solar cells based on perovskite/NiO-graphene composites and NiO interface with 25.9 mA/cm2 photocurrent density and 20.8% efficiency. *Nano Energy*, *79*, Article 105452. https://doi.org/10.1016/j.nanoen.2020.105452

Mali, S. S., Kim, H., Kim, H. H., Shim, S. E., & Hong, C. K. (2018). Nanoporous p-type NiOx electrode for pin inverted perovskite solar cell toward air stability. *Materials Today*, *21*(5), 483-500. https://doi.org/10.1016/j.mattod.2017.12.002

Mandadapu, U., Vedanayakam, S. V., Thyagarajan, K., Reddy, M. R., & Babu, B. J. (2017). Design and simulation of high efficiency tin halide perovskite solar cell. *International Journal of Renewable Energy Research*, *7*(4), 1603-1612. https://doi.org/10.20508/ijrer.v7i4.6182.g7270

Mekky, A. B. H. (2020). Electrical and optical simulation of hybrid perovskite-based solar cell at various electron transport materials and light intensity. *Annales de Chimie-Science Des Matériaux*, *44*(3), 179-184. https://doi.org/10.18280/acsm.440304

Mishra, A. K., & Shukla, R. K. (2020). Electrical and optical simulation of typical perovskite solar cell by GPVDM software. *Materials Today: Proceedings*, *49*, 3181-3186. https://doi.org/10.1016/j.matpr.2020.11.376

Mohammadi, M. H., Fathi, D., & Eskandari, M. (2021). Light trapping in perovskite solar cells with plasmonic core/shell nanorod array: A numerical study. *Energy Reports*, *7*, 1404-1415. https://doi.org/10.1016/j.egyr.2021.02.071

Mohtasham, J. (2015). Review article-renewable energies. *Energy Procedia*, *74*, 1289-1297. https://doi.org/10.1016/j.egypro.2015.07.774

Mouchou, R. T., Jen, T. C., Laseinde, O. T., & Ukoba, K. O. (2021). Numerical simulation and optimization of p-NiO/n-TiO_2 solar cell system using SCAPS. *Materials Today: Proceedings*, *38*, 835-841. https://doi.org/10.1016/j.matpr.2020.04.880

Mulik, R. N. (2019). Microstructural studies of nanocrystalline nickel oxide. *International Journal of Research and Analytical Reviews*, *6*(2), 973-981.

Nam, Y. M., Huh, J., & Jo, W. H. (2010). Optimization of thickness and morphology of active layer for high performance of bulk-heterojunction organic solar cells. *Solar Energy Materials and Solar Cells*, *94*(6), 1118-1124. https://doi.org/10.1016/j.solmat.2010.02.041

Nkele, A. C., Nwanya, A. C., Shinde, N. M., Ezugwu, S., Maaza, M., Shaikh, J. S., & Ezema, F. I. (2020). The use of nickel oxide as a hole transport material in perovskite solar cell configuration: Achieving a high performance and stable device. *International Journal of Energy Research*, *44*(13), 9839-9863. https://doi.org/10.1002/er.5563

Pindolia, G., Shinde, S. M., & Jha, P. K. (2022). Optimization of an inorganic lead free $RbGeI_3$ based perovskite solar cell by SCAPS-1D simulation. *Solar Energy*, *236*, 802-821. https://doi.org/10.1016/j.solener.2022.03.053

Reyes, A. C. P., Lázaro, R. C. A., Leyva, K. M., López, J. A. L., Méndez, J. F., Jiménez, A. H. H., Zurita, A. L. M., Carrillo, F. S., & Durán, E. O. (2021). Study of a lead-free perovskite solar cell using CZTS as HTL to achieve a 20% PCE by SCAPS-1D simulation. *Micromachines*, *12*(12), Article 1508. https://doi.org/10.3390/mi12121508

Ragb, O., Mohamed, M., Matbuly, M. S., & Civalek, O. (2021). An accurate numerical approach for studying perovskite solar cells. *International Journal of Energy Research, 45*(11), 16456-16477. https://doi.org/10.1002/er.6892

Rahman, M. S., Miah, S., Marma, M. S. W., & Sabrina, T. (2019). Simulation based investigation of inverted planar perovskite solar cell with all metal oxide inorganic transport layers. In *2019 International Conference on Electrical, Computer and Communication Engineering (ECCE)* (pp. 1-6). IEEE Publishing. https://doi.org/10.1109/ECACE.2019.8679283

Rai, M., Wong, L. H., & Etgar, L. (2020). Effect of perovskite thickness on electroluminescence and solar cell conversion efficiency. *The Journal of Physical Chemistry Letters*, *11*(19), 8189-8194. https://doi.org/10.1021/acs.jpclett.0c02363

Rai, S., Pandey, B. K., Garg, A., & Dwivedi, D. K. (2021). Hole transporting layer optimization for an efficient lead-free double perovskite solar cell by numerical simulation. *Optical Materials*, *121*, Article 111645. https://doi.org/10.1016/j.optmat.2021.111645

Ravishankar, S., Aranda, C., Sanchez, S., Bisquert, J., Saliba, M., & Garcia-Belmonte, G. (2019). Perovskite solar cell modeling using light-and voltage-modulated techniques. *The Journal of Physical Chemistry C*, *123*(11), 6444–6449. https://doi.org/10.1021/acs.jpcc.9b01187

Said, N. D. M., & Woon, L. C. (2019). Fill factor and power conversion efficiency simulation of heterojunction organic solar cells (P_3HT/PCBM) using ZnO and PEDOT: PSS as interfacial layer. *International Journal of Advanced Research in Technology and Innovation*, *1*(2), 64-71.

Samanta, M., Ahmed, S. I., Chattopadhyay, K. K., & Bose, C. (2020). Role of various transport layer and electrode materials in enhancing performance of stable environment-friendly Cs_2TiBr_6 solar cell. *Optik*, *217*, Article 164805. https://doi.org/10.1016/j.ijleo.2020.164805

Danjumma, S. G., Abubakar, Y., & Suleiman, S. (2019). Nickel Oxide (NiO) Devices and Applications: A Review. *International Journal of Engineering Research & Technology*, *8*(04), 461-467. https://doi.org/10.17577/ijertv8is040281

Schileo, G., & Grancini, G. (2021). Lead or no lead? Availability, toxicity, sustainability and environmental impact of lead-free perovskite solar cells. *Journal of Materials Chemistry C*, *9*(1), 67-76. https://doi.org/10.1039/D0TC04552G

Shamna, M. S., Nithya, K. S., & Sudheer, K. S. (2020). Simulation and optimization of $CH_3NH_3SnI_3$ based inverted perovskite solar cell with NiO as Hole transport material. *Materials Today: Proceedings*, *33*, 1246-1251. https://doi.org/10.1016/j.matpr.2020.03.488

Shyma, A. P., & Sellappan, R. (2021). *Computational probing of tin-based lead-free perovskite solar cells: Effects of absorber parameters and various ETL materials on device performance*. ResearchSquare. https://doi.org/10.21203/rs.3.rs-658718/v1

Sievers, D. W., Shrotriya, V., & Yang, Y. (2006). Modeling optical effects and thickness dependent current in polymer bulk-heterojunction solar cells. *Journal of Applied Physics*, *100*(11), Article 114509. https://doi.org/10.1063/1.2388854

Singh, A. K., Srivastava, S., Mahapatra, A., Baral, J. K., & Pradhan, B. (2021). Performance optimization of lead free-$MASnI_3$ based solar cell with 27% efficiency by numerical simulation. *Optical Materials*, *117*, Article 111193. https://doi.org/10.1016/j.optmat.2021.111193

Sittirak, M., Ponrat, J., Thubthong, K., Kumnorkaew, P., Lek-Uthai, J., & Infahsaeng, Y. (2019). The effects of layer thickness and charge mobility on performance of FAI: MABr: PbI_2: $PbBr_2$ perovskite solar cells: GPVDM simulation approach. In *Journal of Physics: Conference Series* (Vol. 1380, No. 1, p. 012146). IOP Publishing. https://doi.org/10.1088/1742-6596/1380/1/012146

Song, T. B., Yokoyama, T., Aramaki, S., & Kanatzidis, M. G. (2017). Performance enhancement of lead-free tin-based perovskite solar cells with reducing atmosphere-assisted dispersible additive. *ACS Energy Letters*, *2*(4), 897-903. https://doi.org/10.1021/acsenergylett.7b00171

Soucase, B. M., Baig, F., Khattak, Y. H., Vega, E., & Mollar, M. (2022). Numerical analysis for efficiency limits of experimental perovskite solar cell. *Solar Energy*, *235*, 200-208. https://doi.org/10.1016/j.solener.2022.02.051

Srivastava, M., Singh, P. K., Gultekin, B., & Singh, R. C. (2021). Fabrication of room ambient perovskite solar cell using nickel oxide HTM. *Materials Today: Proceedings*, *34*, 748-751. https://doi.org/10.1016/j.matpr.2020.04.688

Sun, P. P., Li, Q. S., Yang, L. N., & Li, Z. S. (2016). Theoretical insights into a potential lead-free hybrid perovskite: substituting Pb^{2+} with Ge^{2+}. *Nanoscale*, *8*(3), 1503-1512. https://doi.org/10.1039/c5nr05337d

Thakur, U. K., Kumar, P., Gusarov, S., Kobryn, A. E., Riddell, S., Goswami, A., Alam, K. M., Savela, S., Kar, P., Thundat, T., Meldrum, A., & Shankar, K. (2020). Consistently high V oc values in pin type perovskite solar cells using Ni^{3+}-Doped NiO nanomesh as the hole transporting layer. *ACS Applied Materials & Interfaces*, *12*(10), 11467-11478. https://doi.org/10.1021/acsami.9b18197

Then, F. S. X., Azhari, A. W., Halin, D. S. C., Sepeai, S., & Ludin, N. A. (2021). Simulation studies on thickness variation of perovskite absorption layer for solar cells application. In *AIP Conference Proceedings of Green Design and Manufacture* (Vol. 2339, No. 1, Article 020071). AIP Publishing. https://doi.org/10.1063/5.0044580

Vishnuwaran, M., Ramachandran, K., & Roy, P. (2022). SCAPS simulated FASnI3 and MASnI3 based PSC solar cells: A comparison of device performance. In I*OP Conference Series: Materials Science and Engineering* (Vol. 1219, No. 1, Article 012048). IOP Publishing. https://doi.org/10.1088/1757-899X/1219/1/012048

Wang, Q., Phung, N., Di Girolamo, D., Vivo, P., & Abate, A. (2019). Enhancement in lifespan of halide perovskite solar cells. *Energy & Environmental Science*, *12*(3), 865-886. https://doi.org/10.1039/c8ee02852d

Wang, R., Mujahid, M., Duan, Y., Wang, Z.-K., Xue, J., & Yang, Y. (2019). A review of perovskites solar cell stability. *Advanced Functional Materials*, *29*(47), Article 1808843. https://doi.org/10.1002/adfm.201808843

Xi, Q., Gao, G., Zhou, H., Zhao, Y., Wu, C., Wang, L., Lei, Y., & Xu, J. (2019). Highly efficient inverted perovskite solar cells mediated by electrodeposition-processed NiO NPs hole-selective contact with different energy structure and surface property. *Applied Surface Science*, *463*, 1107-1116. https://doi.org/10.1016/j.apsusc.2018.09.019

Yang, G., Wang, C., Lei, H., Zheng, X., Qin, P., Xiong, L., Zhao, X., Yan, Y., & Fang, G. (2017). Interface engineering in planar perovskite solar cells: Energy level alignment, perovskite morphology control and high performance achievement. *Journal of Materials Chemistry A*, *5*(4), 1658-1666. https://doi.org/10.1039/c6ta08783c

Yang, H., Park, H., Kim, B., Park, C., Jeong, S., Chae, W. S., Kim, W., Jeong, M., Ahn, T. K., & Shin, H. (2021). Unusual hole transfer dynamics of the NiO layer in methylammonium lead tri-iodide absorber solar cells. *The Journal of Physical Chemistry Letters*, *12*(11), 2770-2779. https://doi.org/https://doi.org/10.1021/acs.jpclett.1c00335

Yasodharan, R., Senthilkumar, A. P., Ajayan, J., & Mohankumar, P. (2019). Effects of layer thickness on Power Conversion Efficiency in Perovskite solar cell: A numerical simulation approach. In *2019 5th International Conference on Advanced Computing and Communication Systems, ICACCS 2019* (pp. 1132-1135). IEEE Publishing. https://doi.org/10.1109/ICACCS.2019.8728410

Yongjin, G., Xueguang, B., Yucheng, L., Binyi, Q., Qingliu, L., Qubo, J., & Pei, M. (2020). Numerical investigation energy conversion performance of tin-based perovskite solar cells using cell capacitance simulator. *Energies*, *13*(22), Article 5907. https://doi.org/https://doi.org/10.3390/en13225907

Zhao, P., Liu, Z., Lin, Z., Chen, D., Su, J., Zhang, C., Zhang, J., Chang, J., & Hao, Y. (2018). Device simulation of inverted CH3NH3PbI3- xClx perovskite solar cells based on PCBM electron transport layer and NiO hole transport layer. *Solar Energy*, *169*, 11-18. https://doi.org/10.1016/j.solener.2018.04.027